Pesticide Biochemistry and Physiology 206 (2024) 106202

Contents lists available at ScienceDirect

Pesticide Biochemistry and Physiology

journal homepage: www.elsevier.com/locate/pest

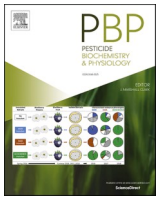

Emamectin benzoate and nanoplastics induce PANoptosis of common carp (*Cyprinus carpio*) gill through MAPK pathway

Zhangyi Ju [a], Yanju Bi [a], Meichen Gao [a], Yilin Yin [a], Tong Xu [a], Shiwen Xu [a,b,*]

[a] College of Veterinary Medicine, Northeast Agricultural University, Harbin 150030, China
[b] Key Laboratory of the Provincial Education, Department of Heilongjiang for Common Animal Disease Prevention and Treatment, College of Veterinary Medicine, Northeast Agricultural, Harbin, 150030, China

ARTICLE INFO

Keywords:
Emamectin benzoate
Nanoplastics
Fish epidermal cells
PANoptosomes
PANoptosis

ABSTRACT

Emamectin benzoate (EMB) is a pesticide that is frequently used. Nanoplastics (NPs) are a recently identified class of pollutants that are ubiquitous in the environment. In the aquatic environment, NPs can appear together with EMB, which may exacerbates the damage to water and aquatic organisms. However, the damage and mechanism of EMB and NPs to the gill tissue of common carp (*Cyprinus carpio*) remain unclear. Therefore, an EMB or/NPs exposure model was constructed to explore the mechanism of EMB or/NPs exposure on carp gill damage. This study was done by immunofluorescence, RT-qPCR, Western blot and other methods. Both *in vitro and in vivo* data indicated that EMB or NPs exposure could lead to gill tissue destruction, oxidative stress with the increased of ROS fluorescence intensity, MDA and H_2O_2 content, and the decreased CAT and GSH-PX activity, and the activation of MAPK pathway. Subsequently, PANoptosomes were activated with the up-regulated mRNA and protein expression of RIPK-1, Caspase-1,NLRP3, ACS, RIPK-3, Caspase-8, resulting in PANoptosis including the increased GSDMD, Caspase-3, MLKL expression. Notably, the results following combined exposure were more pronounced than those observed following exposure alone. The addition of *N*-acetylcysteine (NAC) and 3-methylindole (3-MI) further evidenced that EMB or/and NPs exposure can induce gill damage *via* the ROS/MAPK/PANoptosis pathway. Therefore, the present study reveals that EMB or/NPs exposure induces PANoptosis in carp gill by activating ROS/p38/MAPK signaling.

1. Introduction

In recent years, health problems of pesticide residues have been received more attention in public. Emamectin benzoate (EMB) is a natural product which is isolated from soil microorganisms and belongs to the abamectin family of macrolide pesticides (White et al., 1997). EMB is widely used in agriculture and aquaculture, which easily enter water in many ways (Gu et al., 2023). In addition, EMB has a half-life of 100–400 days in sediments (Benskin et al., 2014; Strachan and Kennedy, 2021). The maritime benthic species *Corophium* and *Arenicola* have residual EMB levels of 0.115 mg/kg and 0.056 mg/kg, respectively (Telfer et al., 2006). Because EMB is lipophilic, it can pass through nuclear and cellular membranes more easily, which makes it harmful to mammals (Bi et al., 2023). Consequently, the findings show that the chemical causes mitochondrial apoptosis, which is hazardous in human bronchial epithelial cells (16HBE) (Niu et al., 2020). High doses of EMB have been shown to be neurotoxic in rats (Niu et al., 2020; Noshy and Azouz, 2021). Additionally, a recent study evaluated the genotoxicity and cytotoxicity of EMB to normal human hepatocytes (QSG7701 cell line) *in vitro* (Zhang et al., 2017). It was suggested that EMB exposure caused overproduction of reactive oxygen species (ROS), DNA damage, and aberrant mitochondrial distribution (Wang et al., 2023). In addition, EMB resulted in decreased cell viability, which was accompanied by induced apoptosis of Caco-2 cells, suggesting that EMB was cytotoxic to cultured Caco-2 cells (Yue et al., 2024). Although EMB has been shown to be toxic to a wide range of tissues and cells, the mechanism of EMB toxicity to the gills of common carp *(Cyprinus carpio)* is poorly reported. Given that gill lamellae consist of only a single layer of epithelial cells, fish gill tissue and fish epithelial cells (EPCs) were selected in this study to establish *in vivo and in vitro* models for follow-up studies (Yilong, 1997).

Emerging is the notion of PANoptosis, which emphasizes the coordination and communication among three types of programmed cell death: necrotic apoptosis, apoptosis, and pyroptosis (Malireddi et al.,

* Corresponding author at: College of Veterinary Medicine, Northeast Agricultural University, Harbin 150030, China.
E-mail address: shiwenxu@neau.edu.cn (S. Xu).

https://doi.org/10.1016/j.pestbp.2024.106202
Received 17 August 2024; Received in revised form 16 October 2024; Accepted 31 October 2024
Available online 2 November 2024

2019; Samir et al., 2020). PANoptosome is a key molecule in pyroptosis, apoptosis and/or necrotic apoptosis, while participating in and providing molecular scaffolding (Wang and Kanneganti, 2021). Drp1 has been reported to mediate the production of mitochondrial ROS during the development of glaucoma, leading to the imbalance of the redox system and ultimately PANoptosis (Zeng et al., 2023). Research has found that triptolide-induced PANapoptosis was associated with mitochondrial dysfunction and ROS production (Zhang et al., 2023). In addition, the family of mitogen-activated protein kinases is essential for controlling both apoptosis and cell division. In a study, TLR9 was shown to activate PANapoptosis through the p38/MAPK pathway (Zhou et al., 2022). Study of Lan showed that PANapoptosis induced by cerebral ischaemia-reperfusion (I/R) can be attenuated by upstream regulators of the MAPK pathway (Lan et al., 2024). Moreover, an increase in intracellular ROS leads to activation of ERK, JNK and p38/MAPK (Son et al., 2011). Lactic acid has been shown to adjust ROS, trigger the p38/MAPK signaling pathway, and promote differentiation of C2C12 cell differentiation (Cheng et al., 2024). Secondly, it has been shown that polyphyllin VII can cause HepG2 cells to undergo apoptosis by producing ROS, which in turn causes mitochondrial malfunction and activates the MAPK pathway in response to mitogen-activated protein kinase stimulation (Zhang et al., 2016). Selenium caused neutrophil apoptosis and necrotic apoptosis in carp and reduced the inhibitory effect of tetrabromobisphenol A (TBBPA) on extracellular traps (NETs) release by controlling ROS/MAPK-pathologically (Gong et al., 2023). di-(2-ethylhexyl) phthalic acid (DEHP) can mediate pyroptosis of L8824 cells through the ROS/MAPK/NF-κB signaling pathway (Cai et al., 2023a, 2023b). These findings indicate that stimulation of the ROS/p38/MAPK pathway can cause PANoptosis.

At present, one of the most environmentally dangerous nanomaterials on the market is nanoplastics (NPs) (González-Fernández et al., 2021). Over the past ten years, aquatic ecosystems have also been detected NPs, which are particles smaller than 100 nm (Ter Halle et al., 2017). It has been reported that NPs can affect reproduction, fertilisation, embryogenesis, neuronal and motor activity, and immunity, thereby inducing oxidative stress (González-Fernández et al., 2018; Sendra et al., 2020; Tallec et al., 2020; Zhang et al., 2020). NPs exposure can induce oxidative stress, which in turn activates the MAPK signaling pathway and induces programmed cell death (Wang et al., 2022; Chen et al., 2023a, 2023b). Currently, NPs and EMB contamination often co-occur in the environment (Ye et al., 2022). However, It is unclear that the combination of EMB and NPs exposure on the type of damage to carp gill cells and toxicological damage through the specific mechanism of ROS/P38/ERK/JNK. Therefore, we established the gill tissue and Epithelioma papulosum cyprini (EPC) cell models of EMB/NPs in carp. Cell viability was assessed in relation to EMB and NPs using the CCK-8 technique. The existence of oxidative stress was determined by measuring oxidative stress markers (ROS, MDA, CAT, H_2O_2) and antioxidant enzyme activity (GPx) in the cells. Additionally, to ascertain the precise amount and ratio of necrosis and apoptosis under EMB/NPs by AO/EB and flow cytometry, and western blotting were used to determine the expression levels of genes associated with the P38/ERK/JNK pathway and the PANoptosome complex (NLRP3, ASC, Cas1, Cas8, RIPK-1, RIPK-3). Our research aims to raise public awareness of the dangers that pesticides pose to fish, aquatic life and the environment. It also aims to shed light on the precise relationship between cell damage and combined exposure to EMB and NPs, as well as to offer new insights into the toxicological mechanism of pesticides on the ROS/P38/ERK/JNK axis in fish.

2. Materials and methods

2.1. Carp models

All procedures in this study strictly followed the instructions of the Animal Care and Use Committee (SRM-11) of Northeast Agricultural University. EMB (purity ≥95 %) and NPs (approximately 100 nm, 25 mg/mL) were purchased from Shanghai yuanye Bio-Technology Co., Ltd. and Zhongke Yannuo New Material Technology Co., Ltd., respectively. Sixty healthy carp were randomly divided into four groups: control group, EMB group (2.4 μg/L in water), NPs group (500 μg/L in water), and EMB + NPs group (with drug contents of 2.4 μg/L and 500 μg/L, respectively) (Kumar et al., 2022; Junaid et al., 2024; Abarghouei et al., 2021). The carps were fed twice a day and add EMB and NPs to the water according to the dosage. On the 31st day, each group of carp was euthanized to obtain gill tissue. Subsequently, a portion of the gill samples were washed with ice PBS and fixed in 4 % paraformaldehyde (PFA), while the other portion was stored at −80 °C for other experiments.

2.2. Hematoxylin and eosin (H&E) staining

The gill tissue was fixed for a minimum of 24 h in 4 % paraformaldehyde (Biosharp, China). The gills were cut off ($n = 3$) and stained with H&E.

2.3. The DUTP-biotin notch end marking (TUNEL) test

A TUNEL test kit (C1086, Beyotime) was used for TUNEL staining in accordance with the instructions. The cells were treated with protease K and H_2O_2 respectively. The test was carried out according to Zhao (Zhao et al., 2021) method and reagent manufacturer's instruction. DAPI was used to nucleate fish gills.

2.4. Cell treatment

After removing the fish epidermal cells (EPCs) stored in laboratory liquid nitrogen, immediately immerse the cell freezing tube in sterile solution. The melted cell suspension was placed in L15 medium (11,415,064, Gibco) containing 10 % FBS (1,705,124, VivaCell, Shanghai, China) and 1 % penicillin methicillin (Beyotime, China), and cultured in a constant temperature incubator at 28 °C. The ROS inhibitor *N*-acetyl-l-polyacetate (NAC, A7250) was acquired by Solarbio Technology in China. The activator 3-methylindole (3-MI, HY-W007355) was purchased from MedChemExpress in China.

2.5. Cell counting kit (CCK-8)

Cell viability was measured using a cell counting kit (CCK-8, St. Biotechnology, Shanghai, China). Fish epithelial cells were incubated for 3 h in 96 well plates (5×10^4 cells/mL) at 28 °C. Concentration gradients for EMB and NPs have been determined. The concentration gradient of the EMB is 0, 0.5, 1, 1.5, 2, 2.5, 3, 3.5, and 4 μM. 2 μM EMB was selected as the concentration of exposure (the cell survival rate was 80.127 %). NPs concentration gradient: 0, 10, 30, 50, 70, 90, 110, 130, 150 μg/mL. 70 μg/mL NPs was selected as the concentration of exposure (the cell survival rate was 70.004 %). Select 2 μM EMB for interaction with various NPs concentrations. NPs concentration gradient: 0, 30, 40, 50, 60, 70, 90, and 100 μg/mL. After adding the medium containing the above concentrations of EMB and NP for 24 h, discard the original medium, and the medium containing 10 % CCK-8was inserted into every well. Following 30 min of room temperature incubation, the absorbance of the 96 well plates was measured at 450 nm. The survival rates were as follows: (CT - blank CT) / (control well CT - blank well CT) × 100 %.

2.6. Oxidative stress

The treated gill tissue was collected in a centrifuge tube, centrifuged for 3 min at 3000 rpm/min, and the cells were resuspended with 500 μL PBS. Different groups of gill tissues were measured with ultrasound. The concentration of GSH-PX, CAT, MDA and H_2O_2 were measured with a commercial kit (Nanjing Jiancheng Institute of Biological Engineering).

The gill tissues of different groups were separated by ultrasonic method. Specific tests have been carried out as instructed by the manufacturer.

2.7. ROS test

The ROS kit (Nanjing Jiancheng Institute of Biological Engineering) was used for fluorescence labeling and analysis of ROS in the four groups. After the treatment, the EPC cells in 6 well plates were separated by trypsin without EDTA, and then washed with PBS twice. After 30 min, the EPC cells were again suspended in L15 media with 10 μM DCFH-DA probes. The flow pictures were taken using Thermo Fluorescence Microscopy (USA) and CellSens Standard (OLYMPUS, Japan). Fluorescence intensity was analysed using Image J software.

2.8. Western blot analysis

The target gene expression levels in EPC and gills treated with NPs and EMB were measured using western blot. Four groups of the total extracted proteins were then subjected to electrophoresis (Miao et al.2022). NC membranes received the proteins that had been separated on the surface. After sealing the membrane for 1.5 h at 37 °C in skim milk, the main antibody was left to incubate overnight, and the secondary antibody was left to incubate for 45 min. P38, p-JNK, p-ERK, RIPK-1, RIPK-3, Caspase-3, Caspase-9, MLKL, NLRP3, GSDMD, IL-18 and β-actin were the antibodies used in this investigation shown in Table 1. The strips were then visualized using Azure Imaging Biosystem and ECL (Meilunbio). β-actin served as the reference standard for the analysis of each protein's expression.

2.9. RNA isolation and RT-qPCR

Using the Trizol technique (Takara, Japan), total RNA was extracted. To summarize, each sample was extracted with 1 ml of Trizol, combined with 400 μl of chloroform, and allowed to stand for 8 min before being centrifuged for 15 min to remove the supernatant and add 75 % DEPC ethanol. After centrifuging for 10 min, 40 μL DEPC water was added, and reverse transcription was carried out according to the directions included in the kit (TransGen Biotech). 1 μL of RNA was used for reverse transcription. The sequence of primers is shown in Table 2. The $2^{-\Delta\Delta CT}$ method was used to analyze the relative changes in target gene expression at mRNA level.

2.10. AO/EB staining

The manufacturer's instructions for staining AO/EB were followed when cultivating fish epithelials in L15 media for a full day following treatment (SenBeiJia Biological Technology, Nanjing, China). To summarize, after 15 min of AO/EB solution incubation in the dark, the morphology of both living and dead cells was promptly examined under a fluorescent microscope. After that, ImageJ software was used to calculate the percentage of dead cells.

Table 1
Information of the antibodies used in this study.

Antibody	Dilution ratio	Catalog No.	Resource
NLRP3	1:1500	WL02635	Wanlei, China
ASC	1:500	WL02462	Wanlei, China
Caspase-1	1:500	WL02996	Wanlei, China
Caspase-8	1:1000	WL03426	Wanlei, China
RIPK-1	1:1000	WL04522	Wanlei, China
RIPK-3	1:1000	A5431	Abclonal, China
Caspase-3	1:500	WL04004	Wanlei, China
MLKL	1:500	A5579	Abclonal, China
GSDMD	1:1000	ARC50993	Abclonal, China
P-P38	1:1000	WLP1576	Wanlei, China
P-ERK	1:1000	WLP1512	Wanlei, China
P-JNK	1:1000	WL01813	Wanlei, China
Beta actin	1:10000	ARC5115–01	ABclonal, China

2.11. Flowcytometry

Apoptosis test kit (Jiangsu Kaiji Biotechnology Co., LTD., China). Centrifuged for 5 min at 1000 rpm and washed twice with PBS. The cell pellet was resuspended to 5×10^5/mL in 500 mL. Addition of 5 μL of annexin V-FITC was added to each group, and 5 μL propyl iodide was added in 1 h. Flow cytometric assay (Becton & Dickinson, Franklin, NJ, USA) was used for quantitation of apoptosis, necrosis and viable cell count.

2.12. Hoechst 33342

Hoechst 33342 (product No.C0031; Beijing Sorabio Technology Co., LTD.) was used for 10 min at room temperature. When apoptosis occurs, the nuclei of apoptotic cells are densely stained or fragmented.

2.13. Immunofluorescence staining

The EPC cells underwent a twofold immunofluorescence labeling process. The cells were fixed for one night with 4 % paraformaldehyde, after which they underwent three five-minute washes, one more night of incubation at 4 °C with the first antibody, and then they were again washed with the washing solution. The first antibody was then incubated for 1.5 h at room temperature in dark, followed by two hours at 37 °C, one hour at 25 °C, and five minutes at room temperature with DAPI. NLRP3 (1:200, Ablconal) and GSDMD (1:200, Ablconal) were the main antibodies used. The secondary antibodies used were DAPI (11,000, Biodragon), Dlight 594, and 488.

2.14. Analysis of statistics

The data was analysed and visualized using GraphPad Prism (version 9.0). Results were presented as mean ± standard error of the mean (SEM). We performed the Shapiro-Wilk normality test and found that the data in this article passed the normality trial (alpha = 0.05). The one-way analysis of variance (ANOVA) was used to compare the differences in index among groups. The same letter represents no significant difference ($P > 0.05$); completely different letters represent a significant difference ($P < 0.05$).

3. Results

3.1. Effect of exposure to EMB and/or NPs on gill tissue morphology in common carp and confirmation of in vitro exposure concentrations

First, H&E staining was used to examine how EMB and NPs affected the morphology of common carp gill tissues, as illustrated in Fig. 1A. The gill filament structure was complete and apparent in the CON group, the gill lamels were arranged cleanly and consistently, the epithelial cells and cells that secrete chlorine were arranged thickly and orderly, and the nuclei were evenly distributed and easily visible with no noticeable defects. The gill filaments in the EMB and NPs groups were normal in size and shape, but the epithelial cells of the gill filaments were swollen and sloughed, a small amount of chlorine cells were swollen and necrotic, and the blood vessels were dilated and congested. The combined EMB + NPs group showed obvious vacuolization of cells, disappearance of gill filament structure, fusion and shortening of gill filaments, degeneration and necrosis of epithelial cells, and necrotic changes in chlorine-secreting cells. There was a large amount of inflammatory cell infiltration between the branchial lamellae, and the gap between the branchial lamellae disappeared. These results indicated that EMB and NPs can cause necrosis of gill tissues, and the combination of EMB and NPS can deepen the injury of gill tissues.

Secondly, in Fig. 1B, apoptotic cells with DNA breakage were

Table 2
The RT-qPCR primer for the target gene utilized in this study.

Gene	Forward	Reverse	Efficiency
NLRP3	CCTGGTCTGCTGGATCGTGTG	CGGTGGTGGTCTTGGATGTCTG	95.9 %
ASC	GGACGGAGTGCTGGATGCTTTG	CATCTTGTCGGTGGTCTC	95.5 %
Caspase-1	CTCTGAACTGGGTCTGGCTGAAC	CATTCCTGATCCATCTGGGTCTCTG	96.2 %
Caspase-8	AGTCACAGAGACCAGGAACAAGGAG	TGTAGTAATTGTGCCAGCCGAAGAG	93.6 %
RIPK-1	CACAGGACCGCCACGCAATG	AACACCCAGCAACTTGACCACTC	94.4 %
RIPK-3	AAAGACGAGGACGAGGGAGGAAC	TCGGAGGCTTTGTTGGCTTTGTAG	95.7 %
Caspase-3	CGAGGCCGACAGTGTAAGTGAAG	CAGCGAGAAGATGAACCAGGAACC	92.4 %
MLKL	CTGGTTGACAACGGTCTGAGAGTG	GGTGCTGATTCGTCGGATTGAGG	95.1 %
GSDMD	CATTTGTTAGACGTGGGCACTGAC	CAGCATCAGGCATTTCTTCCATAGC	93.5 %
P38	GCTCAGAGTGGCTTGGATTC	CTTTCAGTGGCTGGAGGTTTA	94.3 %
ERK	CGGCTCACAGCGTAGTCAA	CACCGCAACAGAAGGGAAG	96.1 %
JNK	TGCTTCTGATGGTCGTGTTG	GACTCTTGGCTTTGCACTTTG	94.7 %
β-actin	ACCTGAGCGTAAATACTCTGTCTGG	TCGTCATACTCCTGCTTGCTAATCC	95.8 %

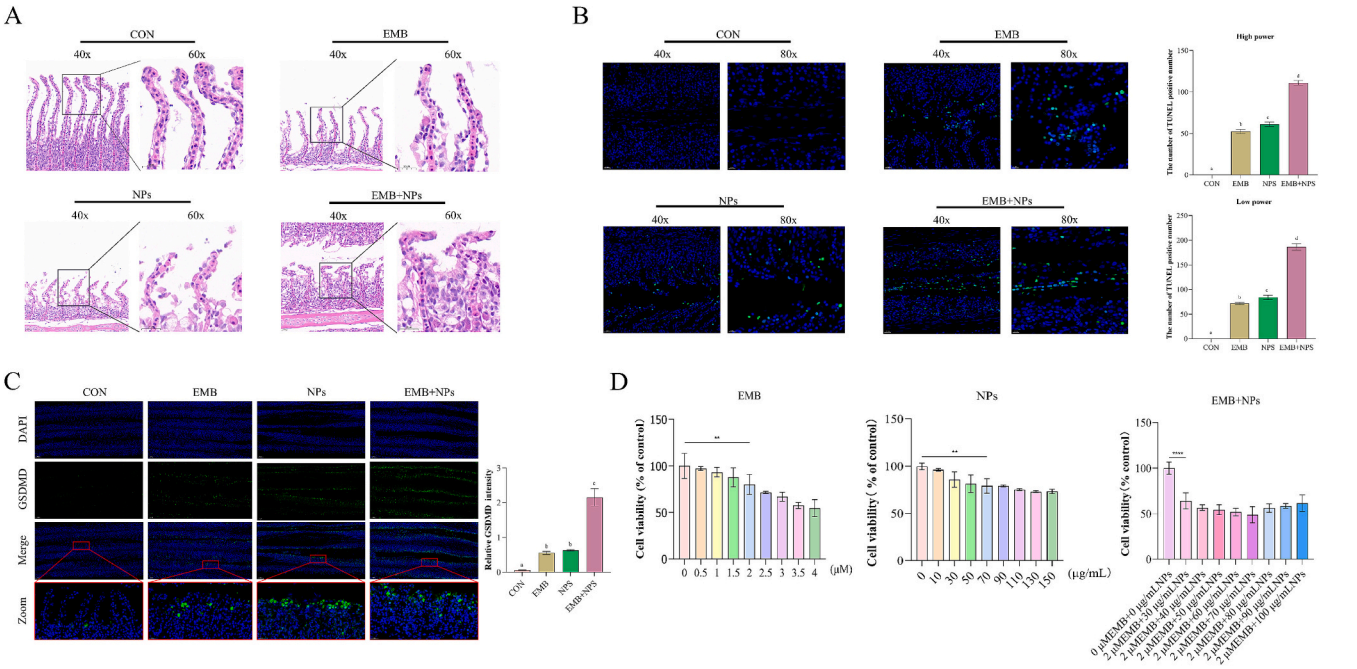

Fig. 1. Observation of gill structure in carp and dosage confirmation of EPC cells exposed to EMB or /NPs. (A) H&E staining results of gills in CON, EMB, NPs and EMB + NPs groups. (B) TUNEL staining results and quantitative analysis of gills in CON, EMB, NPs and EMB + NPs groups ($n = 3$). (C) Pyroptosis staining results and quantitative analysis of gills in CON, EMB, NPs and EMB + NPs groups (n = 3). (D) The viability of EPC cells treated with EMB at different concentrations (0, 0.5, 1, 1.5, 2, 2.5, 3, 3.5 and 4 μM) for 24 h (n = 3); NPs treated EPC cells at different concentrations (0, 10, 30, 50, 70, 90, 110, 130 and 150 μg/mL) for 24 h (n = 3); EPCs exposed to EMB (2 μM) and NPs (0, 30, 40, 50, 60, 70, 80, 90, 100 μg/mL) for 24 h (n = 3). (D) The IC_{50} of EMB and NPs was calculated by nonlinear equation. "*" represents a remarkable difference from the control group ($P < 0.05$).

observed by TUNEL staining. We can see that apoptotic-positive cells were stained green, and quantitative analysis of TUNEL-positive cells was performed. No significant TUNEL-positive cells were found in the CON group. TUNEL-positive gill cells were increased in the EMB and NPs groups, especially at high magnification. Compared to the EMB and NPs groups, there was a significant increase in the quantity of TUNEL-positive kidney cells in the EMB + NPs group.

Pyroptosis staining was then performed in Fig. 1C. Due to the indicative effect of GSDMD on cell apoptosis, we detected the expression level of GSDMD in fish gill tissue. The fluorescence intensity of EMB group or NPs group is higher than that of CON group, and the fluorescence of EMB + NPs group is further enhanced. The results indicate that exposure to EMB and/or NPs leads to pyroptosis in fish gills.

Finally, the CCK8 method was used as a screening dose for EMB and NPs exposure. As shown in Fig. 1D, the activity of EPC cells decreases with increasing concentration of EMB or NPs, indicating a dose-dependent decrease in EPC cell activity with EMB and NP treatment. Finally, we selected 2 μM EMB (survival rate of 80.127 %) and 70 μg/mL NPs (survival rate of 79.004 %) as the *in vitro* exposure doses for this experiment, and 2 μM EMB and 30 μg/mL NPs as the combined toxicity *in vitro* exposure dose (survival rate of 63.847 %). The above results indicate that EMB and/or NPs induce structural integrity and EPC cell damage in carp gill tissue. This damage was most obvious after combined exposure of EMB and NPs, so the EMB + NPs group was used as the representative of the toxic group in subsequent *in vitro* tests.

3.2. The oxidative stress caused by EMB or/and NPs exposure

We first measured the content of MDA and the activity of CAT, GSH-PX, and H_2O_2 in order to assess the degree of oxidative stress in the gill tissues and EPC cells. As shown in Fig. 2A, compared with the control group, the CAT activity of the EMB group, NPs group, and EMB + NPs group decreased, while the levels of MDA and H_2O_2 increased. In terms of GSH, EMB or NPs groups showed a significant decrease in GSH-Px activity. Next, we used EPC cells to confirm the foregoing results *in vitro* in order to confirm their dependability. Intracellular ROS

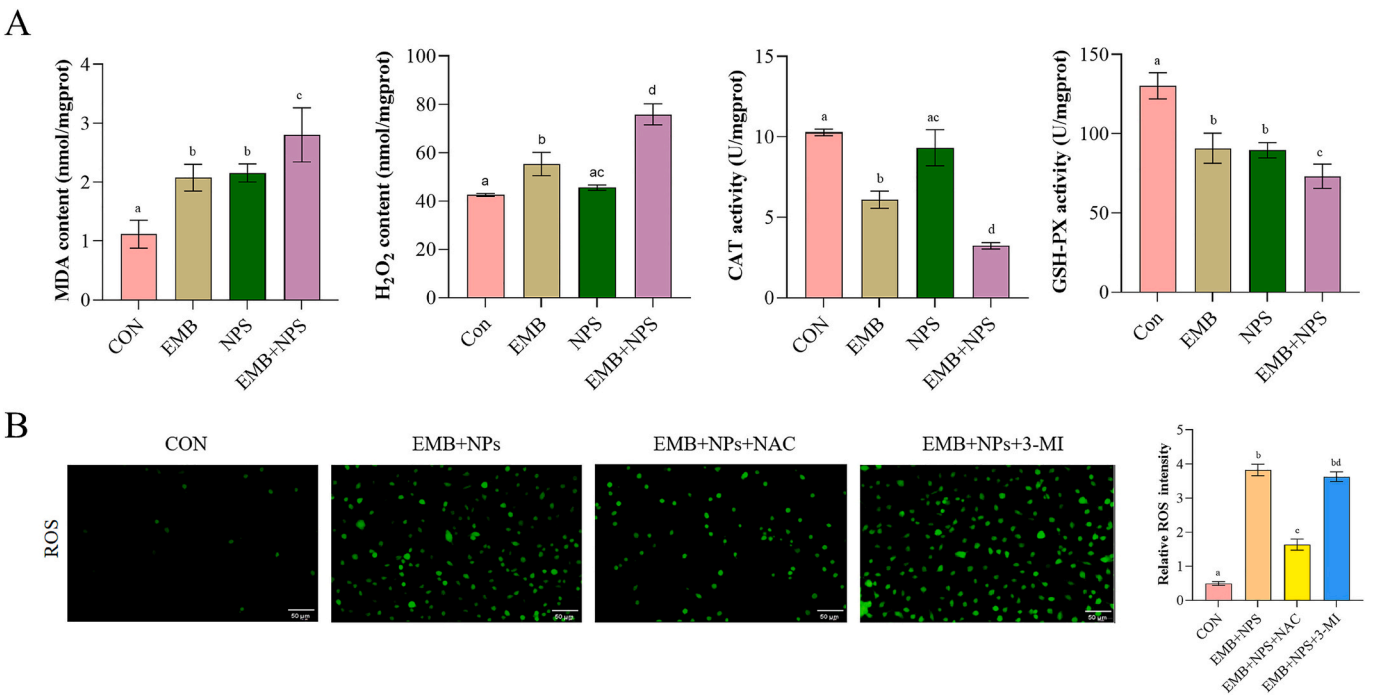

Fig. 2. Effects of EMB and/or NPs exposure on oxidative stress *in vivo and in vitro*. (A) Content of MDA and H_2O_2 and activity of CAT and GSH-Px in gill tissue (n = 3). (B) ROS levels in EPC cells were detected by DCFH-DA staining (green) (scale, 50 μm) (n = 3) and quantification of total fluorescence intensity of ROS in EPC cells (n = 3). (For interpretation of the references to colour in this figure legend, the reader is referred to the web version of this article.)

production was identified and quantified using DCFH probe staining and ImageJ. As demonstrated in Fig. 2B and C, ROS fluorescence intensity were significantly increased in the EMB + NPs group than that in the CON group, but this increase was mitigated in the EMB + NPs + NAC group, which was consistent with the above findings. The findings indicated that EMB and/or NPs caused oxidative stress in carp gill tissue and EPC cells.

3.3. EMB or/and NPs exposure activates the P38/ERK/JNK signaling pathway

Next, We also investigated changes in the MAPK pathway-related genes expression in carp gill tissue and EPC cells. As shown in Fig. 3A and B, EMB or NPs exposure significantly increased protein and mRNA levels in gill tissues compared with the CON group, and this trend was more obvious in the EMB + NPs group (Fig. 3A). At the cellular level, we obtained the same results. More importantly, P38/ERK/JNK-related protein and mRNA expression levels significantly decreased after the addition of NAC combined to the EMB and NPs exposure group. It can be concluded that EMB and NPs activate the MAPK signaling pathway through oxidative stress (Fig. 3B). Taken together, our evidence supports that the exposure to EMB and NPs activated of MAPK signaling pathways both *in vivo and in vitro*.

3.4. Activation of the PAN apoptotic complex by exposure to EMB and/or NPs

To further confirm this hypothesis, changes in the levels of the PANoptosome concluding NLRP3, ASC, Caspase-1, Caspase-8, RIPK-1 and RIPK-3 were detected by Western blotting, immunofluorescence and RT-qPCR *in vivo and in vitro*, as shown in Fig. 4A-B. Within the expected range, the results confirmed an increased signal of the PANoptosome complex with an up-regulation of protein expression levels (NLRP3, ASC, Caspase-1, Caspase-8, RIPK-1 and RIPK-3)and increased mRNA levels after EMB or NPs treatment, the effects of which were exacerbated by the co-exposure to EMB and NPs. This was also confirmed *in vitro*, the study found that the above trend was weakened in the EMB + NP + NAC group after the addition of NAC (Fig. 4B). In conclusion, the exposure of EMB and/or NPs induced PANapoptosis in gill tissue and EPC cells.

3.5. Exposure to EMB and/or NPs induced PANapoptosis in carp gill and EPC cells

As shown in Fig. 5A, gill tissues exposed to EMB and/or NPs showed significantly upregulated protein and mRNA expression levels of Caspase-3, MLKL and GSDMD, and which also was found in EPC cells (Fig. 5B) with the significant upregulation in the EMB + NPs group and a remission in the EMB + NPs + NAC group. As shown in Fig. 5C, AO/EB staining revealed the presence of more bright orange cells representing apoptosis in the other three groups compared to the CON group. Furthermore, these changes were more pronounced in the EMB + NPs group. Moreover, apoptosis was found by flow cytometry, as shown in Fig. 5D. The cells were analysed by flow cytometry using Annexin V-FITC and PI staining. The results of flow cytometry showed that the late apoptosis rates of CON group, EMB + NPs group, EMB + NPs + NAC group and EMB + NPs + 3-MI group were 1.03 %, 11.9 %, 6.66 % and 15.7 %, respectively. The cell necrosis rates were 0.038 %, 7.89 %, 1.26 % and 9.86 %, respectively, indicating that combined exposure to EMB + NPs aggravated apoptosis and necrosis of cells. However, NAC treatment alleviated the damage. Fig. 5E showed that the use of immunofluorescence was used to investigate NLRP3 and GSDMD production. Based on this result, EMB + NPs exposure activated NLRP3 and GSDMD, suggesting that the NLRP3 inflammasome pathway was activated. In addition, NAC blocked the effect of EMB + NPs on the NLRP3 inflammasome pathway, as the expression levels of NLRP3 and GSDMD were attenuated after NAC supplementation. These results suggest that EMB and/or NPs exposure induces PANoptosis in gill tissue and EPC cells, which is exacerbated in the EMB + NPs group. Following staining with Hoechst 33342, cells were studied under fluorescence microscopy, demonstrating a higher proportion of apoptotic cells in the EMB + NPs group compared with the control group. It was discovered that the

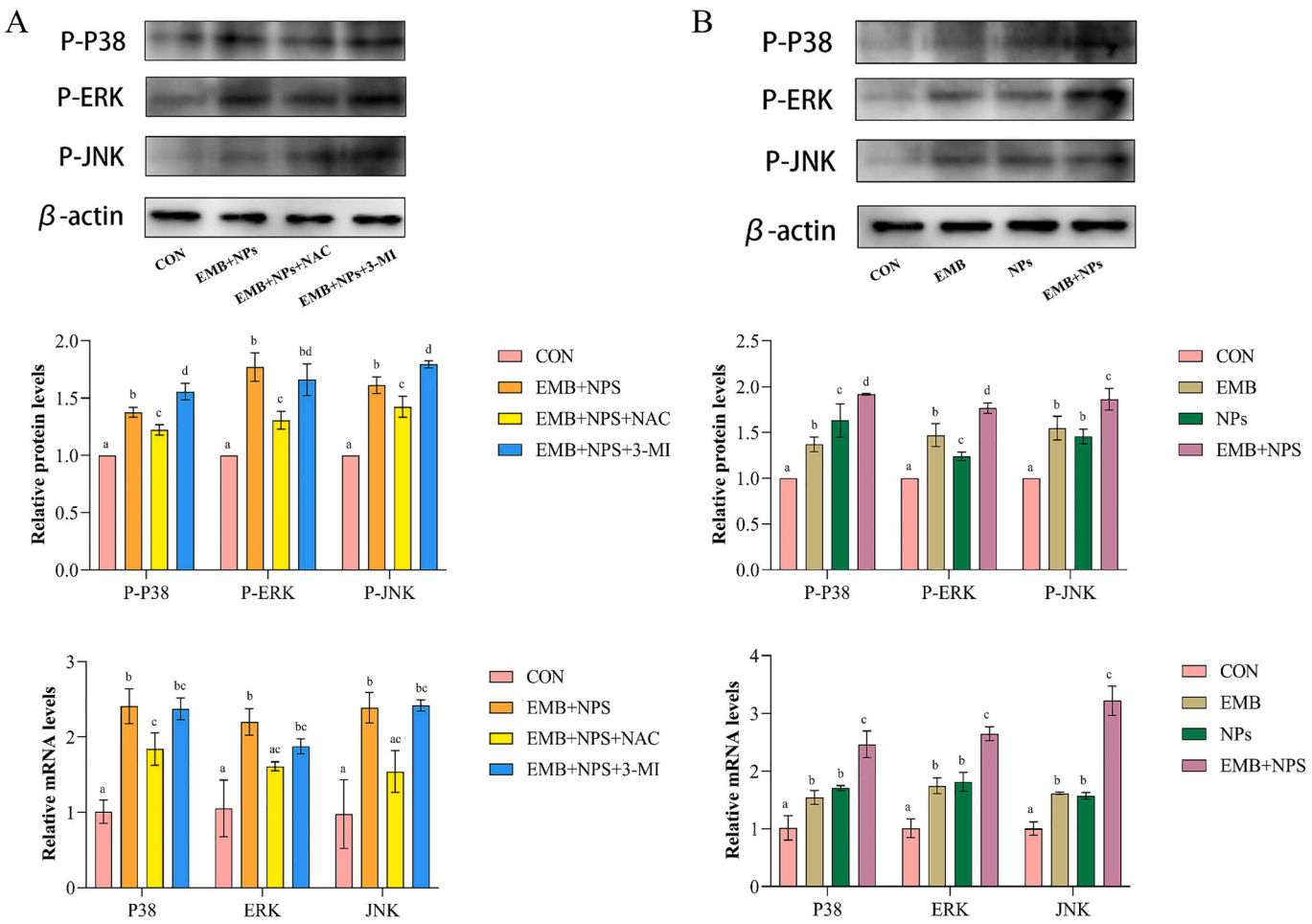

Fig. 3. Effects of EMB or/and NPs exposure on MAPK pathways in EPC cells and fish gill tissues (n = 3). (A) Protein levels and quantitative analysis of P—P38, P-ERK and P-JNK and mRNA quantitative analysis of P38, ERK and JNK genes in EPC cells. (B) Protein levels and quantitative analysis of P—P38, P-ERK and P-JNK in fish gill tissue, and quantitative mRNA analysis of P38, ERK and JNK genes.

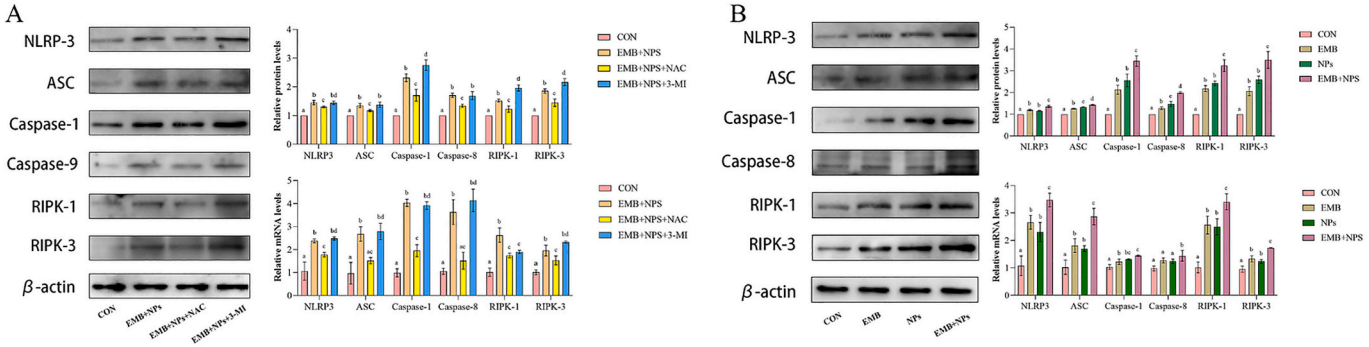

Fig. 4. Effects of EMB and/or NPs exposure on gill tissue and EPC PANoptosome complex (n = 3). (A) Levels and quantitative analysis of PANoptosome complex-related gene proteins and mRNAs in EPC cells. (B) Levels and quantitative analysis of PANoptosome complex related gene protein and mRNA in fish gill tissue.

percentage of apoptotic cells caused by the combination of NPs and EMB was decreased by the addition of NAC (Fig. 5F).

4. Discussion

In recent years, EMB and NPs have become common contaminants, often occurring in the same habitat (Zhang et al., 2022). For example, juveniles of golden mahseer fed an EMB drug diet for 21 days showed histological abnormalities in their intestine, liver, kidney, and muscle tissue (Mallik et al., 2023). NPs can not only enter fish embryo sacs, but also travel through the bloodstream to reach the intestines of adult fish (Ma et al., 2021). Previous studies have confirmed that EMB or NPs can cause cytotoxic changes when exposed to cells separately. Based on this, the present study investigated the mechanism by which EMB and/or NPs induce PANoptosis of fish gill cells through the MAPK pathway and focused on the combined toxicity of EMB and NPs. The findings demonstrated that exposure to EMB or NPs increased the degree of oxidative stress, increased P38, ERK, and JNK mRNA expression and protein levels, activated the PANoptosome complex and increased PANoptosis, and compromised the structural integrity of the gill tissue.

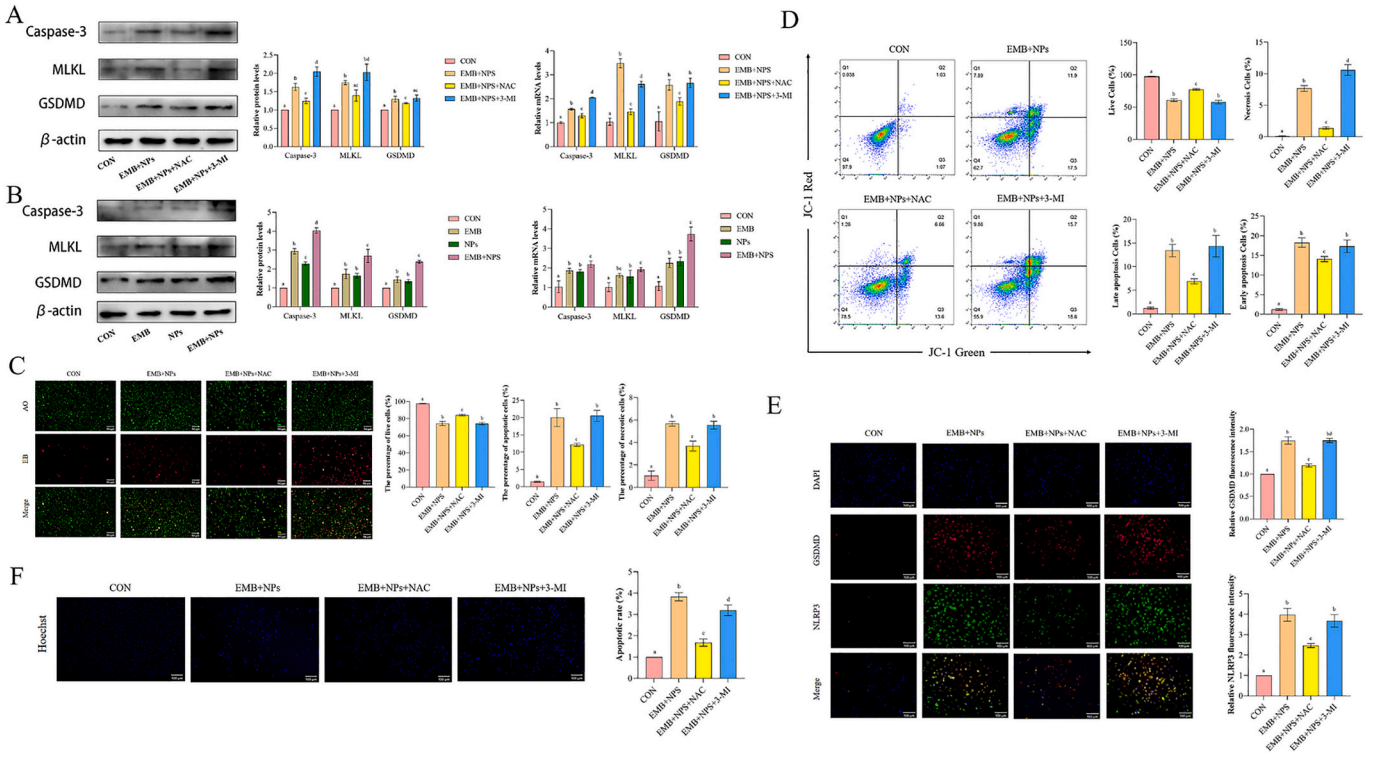

Fig. 5. Effects of EMB or/and NPs exposure on PANoptosis *in vivo and in vitro*. (A) Protein expression and quantification, mRNA level and quantification of Caspase-3, MLKL and GSDMD in EPC cells (n = 3). (B) Protein expression and quantification, mRNA level and quantification of Caspase-3, MLKL and GSDMD in gill tissues (n = 3). (C) Exposure to EMB + NPs and EMB + N AO/EB staining results and quantitative analysis of EPC cells exposed to EMB + NPs + NAC and EMB + NPs + 3-MI. Live cells are bright green, apoptotic cells are bright orange and necrotic cells are red. Count the number of cells with different types of damage from the three randomly selected fields of view and calculate the ratio. (D) Flow cytometry was used to evaluate the effect of EMB and NPs on EPC cell death and the proportion of apoptotic cells in each group. Q1: necrotic cells, Q2: late apoptotic cells, Q3: early apoptotic cells and Q4: normal cells. (E) Immunofluorescence staining of carp EPC cells for NLRP3 (green) and GSDMD (red). DAPI is used to label the nucleus. And quantitative expression levels of NLRP3 and GSDMD. (F) Hoechst33342 staining and quantitative analysis of EPC cells. (For interpretation of the references to colour in this figure legend, the reader is referred to the web version of this article.)

The above results were aggravated after exposure to both. *In vitro* experiments, oxidative stress was inhibited after the addition of NAC and the above processes were alleviated.

Adequate ROS as signaling molecules can support many cellular behaviours, whereas excessive ROS can attack the organism and cause damage (Cheung and Vousden, 2022; Cai et al., 2023a, 2023b; Liu et al., 2023). The zebrafish larvae's head had significantly higher levels of ROS following exposure to EMB, and the antioxidant enzyme CAT and the lipid peroxidation by product MDA were both highly up-regulated (Gu et al., 2023). Furthermore, research has demonstrated that NPs can exacerbate the pro-inflammatory response, cause cell death, and produce ROS. In this work, we verified that the exposure to EMB and NPs resulted disruption of the antioxidant system with elevated CAT, MDA, and H_2O_2 levels and a decrease in Gsh-px. ROS are known to have an activating effect on the MAPK pathway (Yan et al., 2022). For example, cadmium increases the production of ROS and activates the MAPK cell signaling pathway, inducing apoptosis (Cao et al., 2021). In this study, the mRNA transcript levels and protein expression of P38, ERK and JNK were downregulated in EMB and NPs-exposed EPCs when adding NAC. This indicated that exposure to EMB and NPs activated the MAPK pathway by inducing oxidative stress. So far, three upstream molecules of PANoptosis have been identified, namely *Z*-DNA binding protein 1 (ZBP1), RIPK-1, and melanoma 2 (AIM2). They can sense specific stimuli and trigger the assembly of PANoptosome (Gullett et al., 2022). The MAPK pathway's activity is intimately related to the expression of PANoptosome complexes. In addition, p38/MAPK can mediate the TNF-α response by activating RIPK-1 (Lee et al., 2003). PANapoptosis is regulated by the polyprotein PANoptosome complex and is driven by Caspase-8 and RIPK-1 (Pandeya and Kanneganti, 2024). PANoptosome is a complex composed of apoptotic, necrotic and inflammasome components (Samir et al., 2020). PANoptosome induces PANapoptosis in response to various pathogens and endogenous danger signals (Chen et al., 2023a, 2023b). Triptolide induces the activation of pyroptosis, apoptosis and necrotic apoptosis simultaneously and is associated with the co-localisation and interaction of ASC spots with RIPK-3 or Caspase-8, suggesting that the formation of PANoptosome induces PANapoptosis (Zhang et al., 2023). The results of this experiment are consistent with the above studies and the downstream PANoptosome complex is activated by the MAPK pathway. When the MAPK pathway was blocked by NAC, the expression of the RIPK-1-PANoptosome complex in this study was positively correlated with the blocked MAPK pathway. In this study, it can be concluded that after the addition of EMB and NPs, the expressions of pro-apoptotic genes (including Caspase-9 and Caspase-3), necrotic apoptosis-related genes RIPK-1, RIPK-3 and MLKL, and pyroxis-related genes NLRP3, GSDMD and ASC are all upregulated.

Studies have shown that NPs can be used as vehicles to transport contaminants to different aquatic animals, so that aquatic animals are not exposed to just one type of contaminant, which poses multiple threats to the natural aquatic environment (Yu et al., 2021). Compared to NPs and p,p'-DDE (DDE) alone, some cardiac, vascular and immunogenic pathways were significantly downregulated in zebrafish larvae exposed to NPs + DDE (Varshney et al., 2023). Both NPs and DEHP had adverse effects on the male reproductive system in mice. Compared with DEHP alone, the toxic effects of the combined treatment group were enhanced, mainly manifested by decreased sperm quality and structural abnormalities of the testis and epididymis (Li et al., 2022). In this study, we showed that gill damage induced by joint exposure to EMB and NPs was greater than that induced by EMB or NPs alone, revealing a possible

synergistic effect between the two contaminants. In addition, NPs increased EMB-induced ROS overproduction and activated the expression of the MAPK pathway and the PANoptosome complex. These results confirm that EMB and NPs can synergistically enhance the toxic effect on fish gills. By adding NAC and 3-MI to EPC cells, we confirmed that the two toxins activate the MAPK pathway through oxidative stress, exposure to EMB and/or NPs leads to ROS/MAPK pathway in carp gills, thereby inducing PANoptosis.

5. Conclusions

In conclusion, our results demonstrate the synergies that exist between EMB and NPs and suggest a new potential mechanism of EMB and/or NPs exposure for gill damage in common fish. Exposure to EMB or NPs alone can induce overproduction of ROS and activate the MAPK pathway, leading to pan-apoptosis in fish gills. This process is more pronounced in response to combined exposure than to single exposure. The results of this study highlight that co-exposure of EMB and NPs produces more severe toxicity in aquatic animals, providing new insights into the mechanisms of toxicity caused by NPs and other pollutants and broadening the field of toxicological research.

Funding

This research did not receive any specific grant from funding agencies in the public, commercial, or not-for-profit sectors.

CRediT authorship contribution statement

Zhangyi Ju: Writing – original draft, Software, Methodology, Data curation, Conceptualization. **Yanju Bi:** Supervision, Methodology. **Meichen Gao:** Writing – review & editing, Supervision. **Yilin Yin:** Validation, Supervision. **Tong Xu:** Writing – review & editing. **Shiwen Xu:** Writing – review & editing, Resources, Funding acquisition.

Declaration of competing interest

The authors declare that they have no known competing financial interests or personal relationships that could have appeared to influence the work reported in this paper.

Data availability

Data will be made available on request.

Acknowledgements

The authors extend their sincere thanks to the members of the Veterinary Internal Medicine Laboratory and Key Laboratory for Laboratory Animals at the College of Veterinary Medicine, Northeast Agricultural University.

References

Abarghouei, S., Hedayati, A., Raeisi, M., Hadavand, B.S., Rezaei, H., Abed-Elmdoust, A., 2021. Size-dependent effects of microplastic on uptake, immune system, related gene expression and histopathology of goldfish (*Carassius auratus*). Chemosphere 276, 129977.

Benskin, J.P., Ikonomou, M.G., Surridge, B.D., Dubetz, C., Klaassen, E., 2014. Biodegradation potential of aquaculture chemotherapeutants in marine sediments. Aquac. Res.

Bi, Y., Li, X., Wei, H., Xu, S., 2023. Resveratrol improves emamectin benzoate-induced pyroptosis and inflammation of Ctenopharyngodon idellus hepatic cells by alleviating oxidative stress/endoplasmic reticulum stress. Fish Shellfish Immunol. 142, 109148.

Cai, H., Li, K., Yin, Y., Ni, X., Xu, S., 2023a. Quercetin alleviates DEHP exposure-induced pyroptosis and cytokine expression changes in grass carp L8824 cell line by inhibiting ROS/MAPK/NF-κB pathway. Fish Shellfish Immunol. 143, 109223.

Cai, J., Liu, P., Zhang, X., Shi, B., Jiang, Y., Qiao, S., Liu, Q., Fang, C., Zhang, Z., 2023b. Micro-algal astaxanthin improves lambda-cyhalothrin-induced necroptosis and inflammatory responses via the ROS-mediated NF-κB signaling in lymphocytes of carp (*Cyprinus carpio* L.). Fish Shellfish Immunol. 139, 108929.

Cao, X., Fu, M., Bi, R., Zheng, X., Fu, B., Tian, S., Liu, C., Li, Q., Liu, J., 2021. Cadmium induced BEAS-2B cells apoptosis and mitochondria damage via MAPK signaling pathway. Chemosphere 263, 128346.

Chen, J., Chen, X., Xuan, Y., Shen, H., Tang, Y., Zhang, T., Xu, J., 2023a. Surface functionalization-dependent inflammatory potential of polystyrene nanoplastics through the activation of MAPK/ NF-κB signaling pathways in macrophage raw 264.7. Ecotoxicol. Environ. Saf. 251, 114520.

Chen, W., Gullett, J.M., Tweedell, R.E., Kanneganti, T.D., 2023b. Innate immune inflammatory cell death: PANoptosis and PANoptosomes in host defense and disease. Eur. J. Immunol. 53 (11), e2250235.

Cheng, C.F., Li, W.X., Ye, Y.Q., Zhu, Y.J., Tang, M.Y., Hu, Z.H., Su, H., Dang, C.X., Wan, J., Liu, Z.B., Gong, Y.C., Yao, L.H., 2024. Lactate induces C2C12 myoblasts differentiation by mediating ROS/p38 MAPK signalling pathway. Tissue Cell 87.

Cheung, E.C., Vousden, K.H., 2022. The role of ROS in tumour development and progression. Nat. Rev. Cancer 22 (5), 280–297.

Gong, D., Sun, K., Yin, K., Wang, X., 2023. Selenium mitigates the inhibitory effect of TBBPA on NETs release by regulating ROS/MAPK pathways-induced carp neutrophil apoptosis and necroptosis. Fish Shellfish Immunol. 132, 108501.

González-Fernández, C., Tallec, K., Le Goïc, N., Lambert, C., Soudant, P., Huvet, A., Suquet, M., Berchel, M., Paul-Pont, I., 2018. Cellular responses of Pacific oyster (Crassostrea gigas) gametes exposed *in vitro* to polystyrene nanoparticles. Chemosphere 208, 764–772.

González-Fernández, C., Díaz Baños, F.G., Esteban, M., Cuesta, A., 2021. Functionalized nanoplastics (NPs) increase the toxicity of metals in fish cell lines. Int. J. Mol. Sci. 22 (13).

Gu, J., Guo, L., Zhu, Y., Qian, L., Shi, L., Zhang, H., Ji, G., 2023. Neurodevelopmental toxicity of Emamectin benzoate to the early life stage of zebrafish larvae (*Danio rerio*). Int. J. Mol. Sci. 24 (4).

Gullett, J.M., Tweedell, R.E., Kanneganti, T.D., 2022. It's all in the PAN: crosstalk, plasticity, redundancies, switches, and interconnectedness encompassed by PANoptosis underlying the totality of cell death-associated biological effects. Cells 11 (9).

Junaid, M., Liu, S., Liao, H., Yue, Q., Wang, J., 2024. Environmental nanoplastics quantification by pyrolysis-gas chromatography-mass spectrometry in the Pearl River, China: first insights into spatiotemporal distributions, compositions, sources and risks. J. Hazard. Mater. 476, 135055.

Kumar, V., Swain, H.S., Das, B.K., Roy, S., Upadhyay, A., Ramteke, M.H., Kole, R.K., Banerjee, H., 2022. Assessment of the effect of sub-lethal acute toxicity of Emamectin benzoate in Labeo rohita using multiple biomarker approach. Toxicol. Rep. 9, 102–110.

Lan, Z., Tan, F., He, J., Liu, J., Lu, M., Hu, Z., Zhuo, Y., Liu, J., Tang, X., Jiang, Z., Lian, A., Chen, Y., Huang, Y., 2024. Curcumin-primed olfactory mucosa-derived mesenchymal stem cells mitigate cerebral ischemia/reperfusion injury-induced neuronal PANoptosis by modulating microglial polarization. Phytomed.: Intern. J. Phytother. Phytopharmacol. 129, 155635.

Lee, T.H., Huang, Q., Oikemus, S., Shank, J., Ventura, J.J., Cusson, N., Vaillancourt, R.R., Su, B., Davis, R.J., Kelliher, M.A., 2003. The death domain kinase RIP1 is essential for tumor necrosis factor alpha signaling to p38 mitogen-activated protein kinase. Mol. Cell. Biol. 23 (22), 8377–8385.

Li, D., Sun, W., Jiang, X., Yu, Z., Xia, Y., Cheng, S., Mao, L., Luo, S., Tang, S., Xu, S., Zou, Z., Chen, C., Qiu, J., Zhou, L., 2022. Polystyrene nanoparticles enhance the adverse effects of di-(2-ethylhexyl) phthalate on male reproductive system in mice. Ecotoxicol. Environ. Saf. 245, 114104.

Liu, H., Wang, K., Han, D., Sun, W., Xu, S., 2023. Co-exposure of avermectin and imidacloprid induces DNA damage, pyroptosis, and immune dysfunction in epithelioma papulosum cyprini cells via ROS-mediated Keap1/Nrf2/TXNIP axis. Fish Shellfish Immunol. 140, 108985.

Ma, C., Chen, Q., Li, J., Li, B., Liang, W., Su, L., Shi, H., 2021. Distribution and translocation of micro- and nanoplastics in fish. Crit. Rev. Toxicol. 51 (9), 740–753.

Malireddi, R.K.S., Kesavardhana, S., Kanneganti, T.D., 2019. ZBP1 and TAK1: master regulators of NLRP3 Inflammasome/Pyroptosis, apoptosis, and necroptosis (PAN-optosis). Front. Cell. Infect. Microbiol. 9, 406.

Mallik, S.K., Singh, S., Shahi, N., Patil, P.K., Kala, K., Pathak, R., Giri, A.K., Das, P., Tandel, R.S., Chandra, S., Krishna, N., Ravindran, R., Pandey, P.K., 2023. Biosafety, histological alterations and residue depletion of feed administered anti-parasitic drug emamectin benzoate in golden mahseer, tor putitora (Hamilton, 1822) as a model candidate fish for sport fishery and conservation in temperate waters. Front. Pharmacol. 14, 1106124.

Niu, C., Wang, C., Wu, G., Yang, J., Wen, Y., Meng, S., Lin, X., Pang, X., An, L., 2020. Toxic effects of the Emamectin benzoate exposure on cultured human bronchial epithelial (16HBE) cells. Environ. Pollut. 257, 113618.

Noshy, P.A., Azouz, R.A., 2021. Neuroprotective effect of hesperidin against emamectin benzoate-induced neurobehavioral toxicity in rats. Neurotoxicol. Teratol. 86, 106981.

Pandeya, A., Kanneganti, T.D., 2024. Therapeutic potential of PANoptosis: innate sensors, inflammasomes, and RIPKs in PANoptosomes. Trends Mol. Med. 30 (1), 74–88.

Samir, P., Malireddi, R.K.S., Kanneganti, T.D., 2020. The PANoptosome: a deadly protein complex driving Pyroptosis, apoptosis, and necroptosis (PANoptosis). Front. Cell. Infect. Microbiol. 10, 238.

Sendra, M., Saco, A., Yeste, M.P., Romero, A., Novoa, B., Figueras, A., 2020. Nanoplastics: from tissue accumulation to cell translocation into Mytilus

galloprovincialis hemocytes. Resilience of immune cells exposed to nanoplastics and nanoplastics plus Vibrio splendidus combination. J. Hazard. Mater. 388, 121788.
Son, Y., Cheong, Y.-K., Kim, N.-H., Chung, H.-T., Kang, D.G., Pae, H.-O., 2011. Mitogen-activated protein kinases and reactive oxygen species: how can ROS activate MAPK pathways? J. Signal Transduct. 2011, 792639.
Strachan, F., Kennedy, C.J., 2021. The environmental fate and effects of anti-sea lice chemotherapeutants used in salmon aquaculture. Aquaculture 544.
Tallec, K., Paul-Pont, I., Boulais, M., Le Goïc, N., González-Fernández, C., Le Grand, F., Bideau, A., Quéré, C., Cassone, A.L., Lambert, C., Soudant, P., Huvet, A., 2020. Nanopolystyrene beads affect motility and reproductive success of oyster spermatozoa (*Crassostrea gigas*). Nanotoxicology 14 (8), 1039–1057.
Telfer, T.C., Baird, D.J., McHenery, J.G., Stone, J., Sutherland, I., Wislocki, P., 2006. Environmental effects of the anti-sea lice (Copepoda: Caligidae) therapeutant emamectin benzoate under commercial use conditions in the marine environment. Aquaculture 260 (1–4), 163–180.
Ter Halle, A., Jeanneau, L., Martignac, M., Jardé, E., Pedrono, B., Brach, L., Gigault, J., 2017. Nanoplastic in the North Atlantic subtropical gyre. Environ. Sci. Technol. 51 (23), 13689–13697.
Varshney, S., Gora, A.H., Kiron, V., Siriyappagouder, P., Dahle, D., Kögel, T., Ørnsrud, R., Olsvik, P.A., 2023. Polystyrene nanoplastics enhance the toxicological effects of DDE in zebrafish (*Danio rerio*) larvae. Sci. Total Environ. 859 (Pt 2), 160457.
Wang, X., Zhang, X., Sun, K., Wang, S., Gong, D., 2022. Polystyrene microplastics induce apoptosis and necroptosis in swine testis cells via ROS/MAPK/HIF1α pathway. Environ. Toxicol. 37 (10), 2483–2492.
Wang, X., Zhang, M., Zhang, D., Yan, Y., Liu, Q., Xu, C., Zhu, Z., Wu, S., Zong, Y., Cao, Z., Zhang, Y., 2023. Emamectin benzoate exposure impaired porcine oocyte maturation. Theriogenology 206, 123–132.
Wang, Y., Kanneganti, T.D., 2021. From pyroptosis, apoptosis and necroptosis to PANoptosis: a mechanistic compendium of programmed cell death pathways. Comput. Struct. Biotechnol. J. 19, 4641–4657.
White, S.M., Dunbar, D.M., Brown, R., Cartwright, B., Cox, D., Eckel, C., Jansson, R.K., Mookerjee, P.K., Norton, J.A., Peterson, R.F., 1997. Emamectin Benzoate: A Novel Avermectin Derivative for Control of Lepidopterous Pests in Cotton.
Yan, Y., Huang, J., Huan, C., Li, L., Li, C., 2022. Non-esterified fatty acid induces ER stress-mediated apoptosis via ROS/MAPK signaling pathway in bovine mammary epithelial cells. Metabolites 12 (9).
Ye, X., Liu, M., Zhao, N., Xiao, C., Xu, H., Jia, J., 2022. Targeted delivery of emamectin benzoate by functionalized polysuccinimide nanoparticles for the flowering cabbage and controlling Plutella xylostella. Pest Manag. Sci. 78 (2), 758–769.
Yilong, X., 1997. Histological study on the gills of the freshwater crab, sinopotamon yangtsekiense bott. J. Anhui Normal Univer.(Nat. Sci.). 20 (2), 141–144.
Yu, Y., Mo, W.Y., Luukkonen, T., 2021. Adsorption behaviour and interaction of organic micropollutants with nano and microplastics - a review. Sci. Total Environ. 797, 149140.
Yue, X., Lin, F., Gui, S., Zhang, S., Wu, Z., Xiang, Y., Xiao, T., Xiao, J., Cao, H., Shi, Y., 2024. Emamectin benzoate-induced toxicity affects intestinal epithelial integrity involving apoptosis. Food Chem. Toxicol. 190, 114827.
Zeng, Z., You, M., Fan, C., Rong, R., Li, H., Xia, X., 2023. Pathologically high intraocular pressure induces mitochondrial dysfunction through Drp1 and leads to retinal ganglion cell PANoptosis in glaucoma. Redox Biol. 62, 102687.
Zhang, C., Jia, X., Bao, J., Chen, S., Wang, K., Zhang, Y., Li, P., Wan, J.B., Su, H., Wang, Y., Mei, Z., He, C., 2016. Polyphyllin VII induces apoptosis in HepG2 cells through ROS-mediated mitochondrial dysfunction and MAPK pathways. BMC Complement. Altern. Med. 16, 58.
Zhang, H.R., Li, Y.P., Shi, Z.J., Liang, Q.Q., Chen, S.Y., You, Y.P., Yuan, T., Xu, R., Xu, L. H., Ouyang, D.Y., Zha, Q.B., He, X.H., 2023. Triptolide induces PANoptosis in macrophages and causes organ injury in mice. Apoptosis 28 (11–12), 1646–1665.
Zhang, Q., He, Y., Cheng, R., Li, Q., Qian, Z., Lin, X., 2022. Recent advances in toxicological research and potential health impact of microplastics and nanoplastics *in vivo*. Environ. Sci. Pollut. Res. Int. 29 (27), 40415–40448.
Zhang, R., Silic, M.R., Schaber, A., Wasel, O., Freeman, J.L., Sepúlveda, M.S., 2020. Exposure route affects the distribution and toxicity of polystyrene nanoplastics in zebrafish. Sci. Total Environ. 724, 138065.
Zhang, Z., Zhao, X., Qin, X., 2017. Potential genotoxic and cytotoxicity of emamectin benzoate in human normal liver cells. Oncotarget 8 (47), 82185–82195.
Zhao, X., Li, X., Wang, S., Yang, Z., Liu, H., Xu, S., 2021. Cadmium exposure induces mitochondrial pathway apoptosis in swine myocardium through xenobiotic receptors-mediated CYP450s activation. J. Inorg. Biochem. 217, 111361.
Zhou, R., Ying, J., Qiu, X., Yu, L., Yue, Y., Liu, Q., Shi, J., Li, X., Qu, Y., Mu, D., 2022. A new cell death program regulated by toll-like receptor 9 through p38 mitogen-activated protein kinase signaling pathway in a neonatal rat model with sepsis associated encephalopathy. Chin. Med. J. 135 (12), 1474–1485.